The final publication is available at

https://doi.org/10.1016/j.foodcont.2018.05.004

Additional Information

1 **Antifungal and functional properties of starch-gellan films containing thyme**

2 (***Thymus zygis***) **essential oil**

3

4 Mayra Sapper [1*], Paola Wilcaso [1], M. Pilar Santamarina [2], Josefa Roselló [2], Amparo

5 Chiralt [1]

6 [1] Instituto Universitario de Ingeniería de Alimentos para el Desarrollo, Universitat

7 Politècnica de València, Camino de Vera s/n, 46022 Valencia, Spain.

8 [2] Departamento de Ecosistemas Agroforestales, Universitat Politècnica de València,

9 Camino de Vera s/n, 46022 Valencia, Spain.

10

11 **Abstract**

12 Films based on starch-gellan blends at 9:1 and 8:2 ratios containing emulsified or lecithin

13 encapsulated thyme (*Thymus zygis*) essential oil (EO) (0.25 or 0.5 g/g polymer), were

14 obtained by casting method and characterized as to their structural, functional

15 (mechanical, barrier and optical) and *in vitro* antifungal properties against *Alternaria*

16 *alternata* (AA) and *Botryotinia fuckeliana* (BF). The EO retention during the film

17 formation was also quantified. Lecithin encapsulation of the EO allowed for greater oil

18 retention (45-55%), which enhanced the antifungal activity of the films, which were more

19 effective against BF than AA. All films exhibited high oxygen barrier capacity, while

20 lecithin improved the films water barrier properties and gloss, conferring them with a

21 slightly brownish color. Lecithin also reduced the film stiffness and resistance to break

22 and extensibility. Of the studied formulations, 8:2 S:G films with lecithin-encapsulated

23 EO were very effective at controlling fungal growth, while exhibiting adequate functional

24 properties as packaging/coating materials.

25

28

29 **1. Introduction**

30 Over the last few years, research into packaging has paid greater attention to

31 biodegradable materials to substitute, at least partially, conventional plastics. Of the

[*] Corresponding author: maysap@etsiamn.upv.es (M. Sapper).

packaging films made from polysaccharides, those obtained from starch from different sources (corn, cassava, wheat and others) (Luchese, Spada, & Tessaro, 2017) are the most studied of the bio-based polymers, since starch is renewable, inexpensive and widely available and has good film-forming properties (Souza, Goto, Mainardi, Coelho, & Tadini, 2013). Starch films are transparent, tasteless and odorless and have good oxygen barrier properties. However, these films exhibit some drawbacks, such as the high water sensitivity and retrogradation phenomena, both giving rise to changes in the film barrier and mechanical properties during storage (Amalia Cano, Jiménez, Cháfer, Gónzalez, & Chiralt, 2014). Cassava starch has been extensively used to produce films, and, in order to improve their physical and functional properties, its blending with other biopolymers, hydrophobic substances and/or antimicrobial compounds has been proposed (Acosta, Jiménez, Cháfer, González-Martínez, & Chiralt, 2015; Ghanbarzadeh, Almasi, & Entezami, 2011; Parra, Tadini, Ponce, & Lugão, 2004).

Some gums, such as gellan, also exhibit good film-forming properties, their films being clear and insoluble in cold water (Nieto, 2009). It is an exocellular polysaccharide secreted from the bacterium *Sphingomonas elodea*, and consists of repeating tetrasaccharide units of glucose, glucuronic acid and rhamnose residues joined in a linear chain: [→3)-b-D-glucose-(1→4)-b-D-glucuronic acid-(1→4)-b-D-glucose (1→4)-a-L-rhamnose-(1→]n (Chandrasekaran & Radha, 1995; Fialho et al., 2008; Yang, Paulson, & Nickerson, 2010). Xiao et al. (2011) found that composite starch-gellan films presented improved mechanical and barrier properties, and of various gums tested, 20% starch substitution by gellan gum appeared to be the most effective at improving the mechanical properties and storage stability of the starch films (Kim, Choi, Kim, & Lim, 2014).

Food and packaging industries are paying more and more attention to antimicrobial films and coatings due to consumer demand for minimally processed and preservative-free products. The greatest food losses can be mainly attributed to microbiological alterations, which shorten their shelf life and increase the risk of foodborne illnesses. Then, one of the main interests in active packaging design is the inclusion of substances with antimicrobial and/or antioxidant activity within polymeric matrices. Most of this interest is focused on compounds obtained from natural sources, such as essential oils (EOs), which are Generally Recognised as Safe (GRAS) by the US Food and Drug Administration (Atarés & Chiralt, 2016; Calo, Crandall, O'Bryan, & Ricke, 2015).

The antibacterial activity of different phenol-rich EOs, such as thyme EO, has been reported by several authors (Espitia et al., 2014; Jouki, Mortazavi, Yazdi, & Koocheki,

66   2014; Ruiz-Navajas, Viuda-Martos, Sendra, Perez-Alvarez, & Fernández-López, 2013),

67   but fewer studies analyze the antifungal effect of these compounds (Boubaker et al., 2016;

68   Perdones, Chiralt, & Vargas, 2016; Santamarina, Ibáñez, et al., 2016; Santamarina,

69   Roselló, Giménez, & Blázquez, 2016)

70   However, on top of their potential sensory impact on the coated or packaged product, the

71   inclusion of essential oils in packaging materials has many limitations as they can

72   evaporate or degrade during the film formation due to either the high temperatures in

73   thermoprocessed films or the steam drag evaporation in film casting processes, during the

74   drying step. The encapsulation of essential oils could be a solution to maintain their

75   usefulness for a longer time, through the control release of the compounds. One option to

76   encapsulate hydrophobic compounds in an aqueous dispersion is the use of amphiphilic

77   substances, such as lecithin, which can entrap the compound in liposome structures.

78   Zhang et al. (2012) obtained stable lecithin nanoliposomes by sonication for their

79   incorporation in chitosan films. There have been different studies on the encapsulation of

80   volatile compounds into lecithin nanoliposomes before film preparation in order to

81   mitigate both their losses and their sensory impact. The incorporation of lecithin

82   liposomes containing eugenol or cinnamon leaf essential oil into chitosan films allowed

83   for a high retention ratio of volatile compounds (Valencia-Sullca et al., 2016). Jiménez,

84   Sánchez-González, Desobry, Chiralt, & Tehrany (2014) obtained starch-sodium caseinate

85   films containing encapsulated orange essential oil and limonene.

86   The aim of this study was to obtain and characterize antifungal starch-gellan films by

87   incorporating thyme (*Thymus zygis*) essential oil either in free form (direct

88   emulsification) or encapsulated in lecithin nanoliposomes, by analyzing the structural and

89   functional properties of the cast films, as well as their antifungal activity against

90   *Alternaria alternata* and *Botryotinia fuckeliana*.

91

92   **2. Materials and methods**

93   *2.1. Materials and reagents*

94   To prepare the films, cassava starch (S) (Quimidroga S.A., Barcelona, Spain), gellan gum

95   (G) (Kelcogel F, Premium Ingredients, Murcia, Spain), non-GMO soy lecithin with 45%

96   phosphatidylcholine (L) (Lipoid P45, Lipoid GmbH, Ludwigshafen, Germany), thyme

97   (*Thymus zygis*) essential oil (Plantis, Artesanía Agrícola SA, Barcelona, Spain) (EO) and

98   glycerol (Panreac Química S.A., Barcelona, Spain) were used. P_2O_5 and $Mg(NO_3)_2$ salts

99   and UV-grade ethanol were also supplied by Panreac Química S.A. (Barcelona, Spain).

100

2.2. Preparation of liposome dispersions

Liposomes were obtained following the method proposed by (Valencia-Sullca et al., 2016). Lecithin was dispersed in water (5% w/w) and stirred for at least 4 h at 700 rpm. Thyme essential oil (2.5 or 5% w/w) was incorporated into the lecithin dispersion and two formulations (L and L-EO) were obtained, by using a sonicator (Vibra Cell, Sonics & Materials, Inc. USA) at 20 kHz for 10 min with pulses of 1 s.

2.3. Preparation of film-forming dispersions and films

Films were produced by means of casting, using cassava starch (S) and gellan gum (G) in ratios of 9:1 and 8:2, with glycerol (Gly) as plasticizer (ratio polymer: glycerol 1: 0.25). The glycerol ratio was chosen on the basis of previous studies using glycerol plasticized starch-based films (Cano et al., 2015; Jiménez, Fabra, Talens, & Chiralt, 2012). Thyme essential oil (EO) was added as an antifungal compound in a proportion of 0.25 and 0.5 g of EO/g of polymer in two different forms: by direct emulsification or encapsulated in lecithin liposomes (ratio polymer: lecithin 1: 0.5). The EO and lecithin ratios were established on the basis of previous studies into films containing essential oils, considering the potential losses of the compounds during the film drying step (Acosta et al., 2016; Valencia-Sullca et al., 2016).

For this purpose, S (2% w/w) was dispersed in distilled water and kept at 95 °C for 30 min to induce gelatinization, and G dispersion (2% w/w) was obtained under stirring at 90 °C for 60 min. Afterwards, glycerol was added. The S and G dispersions were mixed in adequate proportions to obtain the dispersions without EO. EO was incorporated, either by direct emulsification or encapsulated in lecithin liposomes. In the first case, the EO was added directly and the dispersions were homogenized for 3 min at 13,500 rpm using a rotor-stator homogenizer (Ultraturrax Yellow Line DL 25 Basic, IKA, Staufen, Germany). For the active dispersion with liposomes, this dispersion was added directly to the initial polymer blend and kept under magnetic stirring for 2 h. A control formulation was also obtained with lecithin liposomes without EO, as a control film. All of the dispersions were degassed by using a vacuum pump (MZ 2C NT, Vacuubrand GmbH + CO KG, Germany).

The following formulations were obtained: starch:gellan (9:1 and 8:2); controls with lecithin (9:1-L and 8:2-L); films with EO, in free form (9:1-EO and 8:2-EO), encapsulated in liposomes (9:1-EO-L and 8:2-EO-L), taking into account the two amounts of EO per g

4

134 of polymer: 0.25 and 0.5. Table 1 shows the different film formulations and their

135 respective solid compositions.

136 The mass of the formulations containing 1.5 g of total solids was spread evenly onto

137 Teflon plates of 150 mm in diameter. The films were dried for approximately 48 h at 25

138 ºC and 45% relative humidity (RH). Dry films could be peeled intact from the casting

139 surface and conditioned for 1 week at 53% RH by using a saturated solution of $Mg(NO_3)_2$

140 at 25 ºC, prior to characterization.

141

142 *2.4. Microstructural and physical properties of films*

143 *2.4.1. Microstructure and EO retention in the films*

144 For the microstructural analysis, the film samples were conditioned in desiccators

145 containing P_2O_5 in order to eliminate the water content; then, the films were immersed in

146 liquid nitrogen to obtain cryofractured cross sections (Valencia-Sullca et al., 2016). All

147 of the samples were mounted on copper stubs and platinum coated. Images were obtained

148 by Field Emission Scanning Electron Microscopy (FESEM) (ZEISS®, model ULTRA

149 55, Germany), using an accelerating voltage of 2 kV.

150 To quantify the retention of the active compound during film formation, a known mass

151 of dried film was placed in glass bottles containing 15 mL of an aqueous solution of UV-

152 grade absolute ethanol 50% (v/v), and kept under stirring at 300 rpm for 24 h at 25 °C.

153 Subsequently, aliquots of the samples were extracted and the absorbance (A) was

154 measured at 275 nm, using a spectrophotometer (Evolution 201 UV-Vis, Thermo Fisher

155 Scientific Inc.), as previously described by Tampau, González-Martinez, & Chiralt

156 (2017). The oil concentration in the films was determined by means of a standard curve

157 obtained with the EO solutions in the same solvent containing between 10 and 120 μg/mL.

158 Blanks for the A measurements were the extract of the corresponding film without EO.

159 The equation obtained for the standard curve was C (μg/mL) = 114.88 A.

160 The film thickness was measured with a digital electronic micrometer (Palmer,

161 COMECTA, Barcelona, Spain) to the nearest 0.001 mm at six random positions.

162

163 *2.4.2. Tensile properties*

164 A universal test Machine (TA.XT plus model, Stable Micro Systems, Haslemere,

165 England) was used to obtain the tensile stress-Henky strain curves, from which the elastic

166 modulus (EM), tensile strength (TS) and elongation at break point (%E) of the films were

167 determined, following ASTM standard method D882 (ASTM, 2001). Film samples (2.5

168 cm x 10 cm), conditioned at 25 ºC and 53% RH for 1 week, were evaluated. Samples

169 were mounted in the film-extension grips of the testing machine and stretched at 50 mm

170 min^{-1} until breaking. At least six replicates were obtained for each sample.

171

2.4.3. Barrier properties

173 The water vapor permeability (WVP) of the films was determined following a

174 modification of the E96-95 gravimetric method (ASTM, 1995), exposing the films to a

175 53-100% RH gradient at 25 ºC. To this end, 5 mL of distilled water (100% RH) were

176 placed in Payne permeability cups (3.5 cm in diameter, Elcometer SPRL, Hermelle/s

177 Argenteau, Belgium), put into pre-equilibrated cabinets containing saturated solutions of

178 $Mg(NO_3)_2$ to generate 53% RH inside the cabinet and with a fan on the top of the cup in

179 order to reduce the resistance to water vapor transport. The permeability measurements

180 were taken by weighing the cups periodically (every 1.5 h for 24 h). Eq. (1), proposed by

181 McHugh, Avena-Bustillos, & Krochta (1993), was used to calculate the vapor pressure

182 on the film's inner surface (p_2).

$$WVTR = \frac{P \cdot D \cdot Ln\left[\frac{(P - p_2)}{(P - p_1)}\right]}{R \cdot T \cdot \Delta z} \tag{1}$$

183 where P, total pressure (atm); D, diffusivity of water through air at 25 ºC (m^2 s^{-1}); R, gas

184 law constant (82.057×10^{-3} m^3 atm kmol^{-1} K^{-1}); T, absolute temperature (K); Δz, mean

185 stagnant air gap height (m), considering the initial and final z value; p_1, water vapor

186 pressure on the solution's surface (atm); and p_2, corrected water vapor pressure on the

187 film's inner surface (atm). Water vapor permeance was calculated using Eq. (2) as a

188 function of p_2 and p_3 (pressure on the film's outer surface in the cabinet). WVP of films

189 was obtained by multiplying permeance by film thickness.

$$WVP = \frac{WVTR}{p_2 - p_3} \cdot thickness \tag{2}$$

190 The oxygen permeability (OP) was analyzed in film samples (50 cm^2) by using an Ox-

191 Tran system (Mocon, Minneapolis, USA), following the standard method D3985-05

192 (ASTM, 2002) at 53% RH and 25 ºC. The films were exposed to pure nitrogen flow on

193 one side and pure oxygen flow on the other side. OP was calculated by dividing the

194 oxygen transmission rate by the difference in oxygen partial pressure between the two

195 sides of the film and multiplying it by the average film thickness. Each film formulation

196 was analyzed in triplicate.

197

198 *2.4.4. Moisture content and water solubility*

199 The moisture content of the films, equilibrated at 53% RH and 25 ℃, was analyzed by

200 using a gravimetric method. The film samples were first dried in a vacuum oven at 60 ˚C

201 (Vacioterm-T, JP Selecta S.A., Barcelona, Spain) for 24 h and afterwards equilibrated in

202 a desiccator containing P_2O_5 to remove any residual moisture. Each film formulation was

203 analyzed in triplicate.

204 To determine the film's water solubility, a modification of the methodology proposed by

205 Núñez-Flores et al. (2012) was applied. The film samples (3 cm x 3 cm), previously

206 conditioned in P_2O_5, were weighed (m_o), immersed in glass containers with 10 mL of

207 distilled water (m_w) and kept at 25 ℃ for 24 h. Afterwards, the samples were filtered and

208 an aliquot of the filtrate was dried at 60 °C for 24 h to constant weight in order to

209 determine the mass ratio of soluble solids per g of water of the filtrate (m_{ss}). The solubility

210 of the films (g soluble solids/100 g dry film) was calculated from the soluble solid content

211 by using Eq. (3).

$$\% S = \frac{(m_{ss} \cdot m_w)}{m_o} \cdot 100 \tag{3}$$

212

213 *2.4.5. Optical properties*

214 The opacity of the films was determined by applying the Kubelka−Munk theory for

215 multiple scattering. A spectrocolorimeter (CM-3600d Minolta Co., Tokyo, Japan) was

216 used to obtain the reflection spectra of the films on a white (R) and black (R_0) background

217 between 400 and 700 nm, as well as the spectrum of the white background used (R_g).

218 From these spectra, the internal transmittance (T_i, a transparency indicator) and R_∞ (the

219 reflectance of an infinitely thick film) were calculated using Eqs. (4 to 7)

$$T_i = \sqrt{(a + R_0)^2 - b^2} \tag{4}$$

$$a = \frac{1}{2}\left[R + \frac{R_0 - R + R_g}{R_0 \cdot R_g}\right] \tag{5}$$

$$b = (a^2 - 1)^{1/2} \tag{6}$$

$$R_\infty = a - b \tag{7}$$

220 Three measurements were taken from each film and three films were considered per

221 formulation. From the R_∞ spectra, the CIE *L*a*b** color coordinates were determined

222 using the 10º observer and the D65 illuminant as reference. Moreover, hue (hab*) and

223 chroma (Cab*) were calculated by using:

7

$$h_{ab}^* = arctg\left(\frac{b^*}{a^*}\right) \qquad (8)$$

$$C_{ab}^* = \sqrt{(a^{*2} + b^{*2})} \qquad (9)$$

224 Gloss was measured using a gloss meter Multi Gloss 268 (Minolta, Langenhagen,
225 Germany) at a 60º angle of incidence following ASTM D523 standard method (ASTM,
226 1999). The film samples were placed on a matte black surface, and nine measurements
227 per formulation were taken on the side of the film that was exposed to the atmosphere
228 during drying.

229

230 *2.5. Antifungal tests*

231 For the *in vitro* assays, stock cultures of *Alternaria alternata* (AA) CECT 20923 and
232 *Botryotinia fuckeliana* (BF) CECT 2100, were supplied by the Colección Española de
233 Cultivo Tipo (CECT, Burjassot, Spain). These were preserved frozen in Agar Potato
234 Dextrose (PDA, Scharlab, Barcelona, Spain), then incubated at 25 ºC until sporulation,
235 and used after 7 days of active growth.

236 The films' antifungal properties against AA and BF were determined in Petri dishes (90
237 mm x 15 mm or 150 mm x 20 mm) containing Potato Dextrose Agar (PDA) growth
238 medium. At least four replicates were obtained for each film formulation. These were
239 inoculated with an 8 mm diameter disc of 7-day old colony on PDA of each fungus and
240 coated using film discs 24 mm in diameter. The plates were incubated in the dark at 25
241 ºC for 7 days. The fungal growth was evaluated by measuring the diameter of the colonies
242 in two perpendicular directions daily. The measurements were corrected with the initial
243 radius of the inoculated colony (4 mm). From the radial growth vs. time curves, the
244 growth rate (slope) and total growth inhibition for a determined time (intercept) were
245 estimated. Mycelial growth inhibition (MGI) was also calculated after 7 days of
246 incubation, using Eq. (10).

$$MGI = \frac{DC - DO}{DC} \times 100 \qquad (10)$$

247 where DC is the average diameter of the colonies in the respective control plates (without
248 EO); DO, the average diameter of colonies in the plates containing the active films (with
249 EO).

250

251 *2.6. Statistical analysis*

The statistical analyses of the results were performed through an analysis of variance (ANOVA) and simple linear regression analyses done using Statgraphics Centurion XVI software (Manugistics Corp., Rockville, Md.). Fisher's least significant difference (LSD) procedure was used at the 95% confidence level.

3. Results and discussion

3.1. Microstructure and EO final retention in the films

The functional properties of the films, such as tensile, barrier and optical properties, are directly related to their microstructure and are affected by the interactions between the film components and the drying conditions (Acosta et al., 2016; Song, Zuo, & Chen, 2018). Fig. 1 shows the FESEM images corresponding to the cross-sections of the studied films. S:G blend films, especially in a ratio of 9:1, revealed two layers of differing morphologies which evidenced the partial polymer compatibility and phase separation during the film drying step: one gellan-rich phase (lower in density) on the top and another phase, where starch predominates, at the bottom. The greater viscosity of S:G in a ratio of 8:2 mitigated the phase separation and more homogeneous films were obtained. In films containing lecithin (S:G-L), a multilayer structure was obtained by the formation of lecithin lamellar structure, with the loss of the vesicular structure, during the drying step due to the lipotropic mesomorphism of polar lipids (Krog, 1990; Larsson & Dejmek, 1990). These kinds of layered films, when amphiphilic compounds were incorporated into polymer films, were previously observed for different fatty acids in sodium caseinate films (Fabra, Jimenez, Atares, Talens, & Chiralt, 2009; Fabra, Pérez-Masiá, Talens, & Chiralt, 2011).

When the free EO was incorporated at the lowest concentration, no visible drops of oil were observed in the films, which may be attributed to the great losses during film drying, only retaining a small amount bound to the polymer chains. However, big droplets appear in films containing the highest amount of free EO, thus revealing a greater EO retention in the films. On the other hand, when the EO is incorporated as liposomes, lecithin seems to better maintain its vesicular structure, probably due to the interactions of the EO compounds with the liposomal associations, promoting EO retention in the dried films. Bigger lipid particles could be observed for the highest EO proportion, probably due to the greater progression of the destabilization phenomena (flocculation and coalescence)

in the film-forming aqueous emulsions during the film drying step when the EO content increased.

Table 1 shows the theoretical mass fraction of EO added to the film sample, the amount of EO extracted from the different films and the respective retention percentage (with respect to the initial amount) for each sample. A positive aspect of essential oil incorporation as nanoliposomes was the inhibition of oil evaporation during the film drying step, since 42-56% of the incorporated EO was retained in the dried films. Valencia-Sullca et al. (2016) found similar tendencies in films based on chitosan with the addition of lecithin-encapsulated eugenol and cinnamon leaf essential oil. On the other hand, in films with non-encapsulated EO, the EO retention in the film ranged between 4 and 26%, and it is notable that the sample with the highest proportion of gellan and non-encapsulated EO retained more oil during the film drying, probably due to the greater viscosity of the dispersion, which helps to stabilize the emulsion, mainly limiting the creaming of oil droplets to the film surface, where EO quickly evaporates by steam drag effect, in line with water evaporation, as previously reported by (Perdones et al., 2016). Thus, the obtained results show that liposome encapsulation could be a good strategy with which to reduce the EO losses during the film formation process, which coincides with the observations revealed by the microstructural analysis.

Table 1. Nominal mass fraction (X) of the different components in the dried films (P: total polymer, Gly: glycerol, L: lecithin and EO: essential oil) and total amount of EO extracted from dried films, together with the retention percentage (extracted vs. incorporated). Mean values and standard deviation, in brackets.

Sample	X_P	X_{Gly}	X_L	Incorporated EO (g EO/g total solids)	Extracted EO (g EO/g dry film)	% Retained EO in the film
9:1	0.80	0.20	-	-	-	-
8:2	0.80	0.20	-	-	-	-
9:1-L	0.57	0.14	0.29	-	-	-
8:2-L	0.57	0.14	0.29	-	-	-
9:1-0.25	0.67	0.17	-	0.17	0.015 (0.004)[a]	9 (2)[a]
8:2-0.25	0.67	0.17	-	0.17	0.006 (0.003)[a]	4 (2)[b]
9:1-0.25-L	0.50	0.13	0.25	0.13	0.06 (0.01)[c]	44 (8)[cd]
8:2-0.25-L	0.50	0.13	0.25	0.13	0.053 (0003)[c]	42 (2)[c]
9:1-0.5	0.57	0.14	-	0.29	0.029 (0.003)[b]	10 (1)[a]
8:2-0.5	0.57	0.14	-	0.29	0.074 (0.007)[d]	26 (2)[b]
9:1-0.5-L	0.44	0.11	0.22	0.22	0.123 (0.02)[f]	56 (1)[e]
8:1-0.5-L	0.44	0.11	0.22	0.22	0.111 (0.015)[e]	50 (7)[de]

Different superscript letters within the same column indicate significant differences among films (p < 0.05).

309

3.2. Tensile properties

As concerns tensile behavior, Table 2 shows the values of mechanical parameters (EM, TS and %E) where the effect of the film composition can be observed. All the films with the highest proportion of gellan (8:2), with or without lipids, exhibited greater stiffness (EM) than the corresponding 9:1 S:G films, especially those containing the highest proportion of free EO. Nevertheless, they were less extensible, with the exception of the films with the lowest proportion of free EO, which were the most extensible. Then highest proportion of gellan gave rise to stiffer films with reduced extensibility, probably due to the lack of total miscibility of the polymers, which promoted their brittleness.

Incorporating lipids (EO or L) into the films promoted changes depending on the gellan proportion. The EM decreased in the presence of L or EO, so the films became less stiff, depending on the proportion of G in the matrix. In general, for a given matrix, a greater proportion of lipid (L or EO) led to a greater decrease in both the EM and fracture tension and lower extensibility. However, Valencia-Sullca et al. (2016) found an increase in the extensibility of chitosan films in the presence of lecithin. The observed differences can be explained by the specific interactions between lipid associations of lecithin with a negative surface charge and positively charged chains of chitosan, which does not occur with the neutral chains of starch and gellan, when the cohesion forces of the polymer network were reduced. Different studies have shown that the incorporation of essential oils usually reduces the mechanical strength of the films as a result of the promotion of a heterogeneous structure with enhanced discontinuities (Jiménez et al., 2014; Jouki et al., 2014). However, small amounts of lipids may plasticize the polymer matrix by reducing the chain interaction forces, without introducing great discontinuities.

3.3. Barrier properties

The WVP, OP and thickness values of the different films are also shown in Table 2. WVP is a relevant property directly related to the usefulness of films in food applications and should be as low as possible to prevent water transfer. The lowest WVP was obtained for films with the lowest ratio of lecithin-encapsulated EO, regardless of the polymer matrix, followed by the other formulations with L (with and without EO). Therefore, the presence of L and the subsequent formation of the layered structure in the film reduced the water vapor transfer rate, mainly due to the resistance offered by the lipid layers in the film. A

similar effect was observed by Jiménez et al. (2014), for starch films containing lecithin-encapsulated EO.

However, the incorporation of both L or EO implied an increase in the OP due to the hydrophobic nature of lipids, which facilitates oxygen solubility and transfer (Bertan, Tanada-Palmu, Siani, & Grosso, 2005). This increase was greater in the starch-rich matrix with L, although all the films exhibited very low values of OP, as has been observed for starch-based films (Forssell, Lahtinen, Lahelin, & Myllärinen, 2002).

Table 2. Tensile parameters (elastic modulus, EM; tensile strength, TS; percentage elongation, %E), barrier properties (water vapor permeability, WVP; oxygen permeability, OP) and thickness of the films. Mean values and standard deviation, in brackets.

Sample	EM (MPa)	TS (MPa)	E (%)	WVP (g mm KPa^{-1} h^{-1} m^{-2})	OP x 10^{14} (cm^3 m^{-1} s^{-1} Pa^{-1})	Thickness (μm)
9:1	1273 (64)^i	40 (5)^g	4.9 (1.1)^{fg}	6.7 (0.5)^e	2.70 (0.04)^b	71 (3)^{ab}
8:2	1304 (53)^i	24 (5)^{de}	2.1 (0.6)^{ab}	6.2 (0.3)^d	2.324 (0.005)^a	71 (4)^{ab}
9:1-L	799 (35)^e	14 (2)^{bc}	2.0 (0.4)^{ab}	4.2 (0.4)^b	6.6 (0.3)^g	71 (2)^{ab}
8:2-L	878 (13)^f	23 (3)^d	3.2 (0.5)^{cd}	4.2 (0.1)^b	3.3 (0.2)^{cd}	71 (4)^{ab}
9:1-0.25	745 (86)^{de}	27 (1)^e	7.0 (1.0)^h	4.8 (0.5)^c	3.2 (0.1)^c	70 (2)^a
8:2-0.25	991 (87)^g	35 (5)^f	5.5 (1.4)^g	4.6 (0.1)^{bc}	3.43 (0.02)^{cde}	70 (3)^a
9:1-0.25-L	681 (53)^{cd}	13 (1)^b	2.5 (0.4)^{abc}	3.2 (0.2)^a	4.5 (0.1)^f	73 (2)^{abc}
8:2-0.25-L	707 (80)^d	23 (2)^d	4.2 (0.5)^{ef}	3.2 (0.3)^a	3.5 (0.2)^{cde}	76 (3)^{cd}
9:1-0.5	571 (81)^{ab}	15 (1)^{bc}	3.5 (0.7)^{de}	6.2 (0.8)^d	3.8 (0.3)^e	74 (6)^{bcd}
8:2-0.5	1072 (34)^h	16 (3)^c	1.9 (0.2)^a	7.1 (0.1)^e	3.4 (0.1)^{cd}	73 (6)^{abc}
9:1-0.5-L	514 (74)^a	8 (1)^a	2.0 (0.5)^{ab}	4.3 (0.2)^{bc}	3.59 (0.01)^{de}	76 (8)^{cd}
8:2-0.5-L	612(32)^{bc}	15 (1)^{bc}	2.7 (0.3)^{bcd}	4.3 (0.1)^b	3.3 (0.1)^{cd}	78 (7)^d

Different superscript letters within the same column indicate significant differences among films (p < 0.05).

3.4. Moisture content and solubility

The values for the moisture content and the water solubility of films are shown in Table 3. As expected, the incorporation of L or EO decreased the equilibrium moisture of the films, although films with free EO exhibited similar or slightly higher values than the lipid-free matrices. As regards water solubility, film formulations with L either with or without EO, exhibited significantly lower solubility values, although free EO did not reduce the water solubility of the films. As reported by some authors (Jouki et al., 2014; Ojagh, Rezaei, Razavi, & Hosseini, 2010), adding EO to the polymer films can promote the film's solubility or water adsorption capacity, which could be attributed to the

367 reduction in the polymer chain interactions in the network, making the water adsorption
368 and film solubilization easier.
369
370 *3.5. Optical properties*
371 Table 3 also shows the values of the color coordinates (L*, lightness; C_{ab}*, chrome; h_{ab}*,
372 hue) and gloss at 60° of the different films. Due to the typical color of lecithin, films with
373 liposomes were darker, with a more saturated reddish color. Although the lightness was
374 not significantly affected by the incorporation of the active compound, it slightly
375 decreased in the presence of L and EO. In the same way, the hue decreased in the presence
376 of lecithin due to the color contribution of this component. The film gloss increased in
377 matrices with a greater proportion of G, especially after the incorporation of L.
378 Nevertheless, the addition of EO, both in free form or encapsulated, implied a gloss
379 reduction. This can be attributed to an increase in the surface roughness of the film
380 associated with the creaming of the oil drops during the film drying step and the
381 subsequent oil evaporation, which produces surface irregularities (Sánchez-González,
382 Vargas, González-Martínez, Chiralt, & Cháfer, 2009).
383 Fig. 2 shows the spectral distribution curves of the internal transmittance (T_i) of the films.
384 The incorporation of liposomes, with or without EO, reduced the T_i of the films at low
385 wavelengths due to the brown coloration of L. In contrast, the incorporation of free EO
386 slightly promoted the film transparency of both S:G matrices (9:1 and 8:2), which can be
387 explained by the decrease in the film compactness and, therefore, in the global refractive
388 index. This effect was also observed for lecithin-encapsulated EO.
389
390 **Table 3.** Water solubility (S, % of soluble solids in the film), equilibrium moisture content
391 (X_w, g/100 g dry film), color coordinates (lightness, chrome and hue) and gloss (60°) of
392 the films. Mean values and standard deviation, in brackets.

Sample	S (%)	X_w	L*	C_{ab}*	h_{ab}*	Gloss (60°)
9:1	38 (9)[de]	8.2 (0.3)[d]	81(1)[c]	4.7 (0.4)[a]	88.9 (0.4)[g]	13 (1)[d]
8:2	48 (2)[fg]	8.5 (0.1)[d]	80(1)[d]	5.4 (0.2)[b]	87 (1)[e]	21 (5)[e]
9:1-L	24 (1)[abc]	6.2 (0.1)[a]	76.6 (0.2)[b]	23.1 (0.5)[f]	82.7 (0.4)[c]	52(6)[g]
8:2-L	31 (2)[cde]	6.3 (0.1)[ab]	76.7 (0.4)[b]	22.9 (0.3)[f]	81.9 (0.2)[b]	44 (5)[f]
9:1-0.25	70 (17)[h]	8.5 (0.4)[d]	80.7 (0.4)[c]	5.4 (0.4)[b]	88 (1)[f]	10 (1)[bc]
8:2-0.25	71 (5)[h]	8.1 (0.3)[d]	80.7 (0.5)[c]	6.3 (0.4)[c]	86.6 (0.4)[d]	12 (1)[cd]
9:1-0.25-L	29 (4)[bcd]	6.2 (0.1)[a]	73.0 (0.5)[a]	21 (1)[d]	82.6 (0.4)[c]	13 (2)[cd]
8:2-0.25-L	20 (1)[ab]	5.9 (0.3)[a]	72.2 (0.4)[a]	21 (1)[d]	81.8 (0.3)[b]	7 (1)[a]
9:1-0.5	57 (2)[g]	9.7 (1.1)[e]	76 (8)[b]	7 (2)[c]	90 (1)[h]	9 (1)[ab]
8:2-0.5	41 (4)[ef]	9.5 (0.3)[e]	80.3 (0.3)[c]	6.9 (0.3)[c]	87 (1)[e]	8.0 (0.4)[ab]
9:1-0.5-L	15 (1)[a]	7.7 (0.5)[cd]	73 (1)[a]	22.3 (0.4)[e]	79.5 (0.4)[a]	12 (2)[cd]
8:2-0.5-L	25 (2)[abc]	7.1 (0.6)[bc]	72.4 (0.5)[a]	22.2 (0.4)[e]	79.5 (0.3)[a]	7.2 (0.2)[a]

393 Different superscript letters within the same column indicate significant differences
394 among films (p < 0.05).
395
396 *3.6. Antifungal properties*
397 The antifungal effect exhibited by thyme EO varied depending on the formulation and
398 residual content of EO in the films. Fig. 3 shows the radial growth of each fungus (AA
399 and BF) for the control films (without EO) and the films containing EO applied on the
400 culture plate. A linear fungus growth was observed as a function of time for every sample,
401 and the fitted straight lines ($r^2 > 0.872$) were obtained, with the corresponding slope
402 (growth rate) and intercept, related to the total growth inhibition time (t_0) for each fungus.
403 Table 4 shows the obtained values of GR (slope) and the intercept of the fitted straight
404 lines in each case, as well as the estimated value of the total inhibition period (t_0) and the
405 mycelial growth inhibition (MGI) at 7 days. In terms of its antifungal action, it is
406 remarkable that thyme EO was more effective against *B. fuckeliana* than *A. alternata*. In
407 fact, for an EO concentration in the films of 0.074 g/g dried film (16.6 mg per plate or 0.8
408 mg/mL of medium), no growth of *B. fuckeliana* was observed throughout the tested
409 period, thus indicating a total fungicide action. Likewise, GR values were lower for *B.
410 fuckeliana* than for *A. alternata* for a determined EO content in the film. It is remarkable
411 that no notable differences in GR were observed for *A. alternata* fungus for EO contents
412 in the film between 0 and 6-7% (Figure 4), whereas a sharp decrease in GR was observed
413 for higher contents. In general GR values were slightly lower for the 8:2 S:G matrices for
414 a determined EO content. For *B. fuckeliana* a linear decrease of GR as a function of the
415 EO content in the 8:2 S:G matrices was observed, whereas it fluctuated between 2.5-1.1
416 for the 9:1 S:G matrices depending on the EO content or presence of L. In contrast, t_0
417 values rose when the EO content in the films increased. This behavior suggests that the
418 fungal growth was inhibited for a determined time (t_0) when films contained EO in
419 different proportion, but the EO volatilization or the adaptation of the fungi allows for
420 subsequent growth at the same rate as in the control samples (coated with EO-free films).
421 Only above a critical EO concentration, was the development of the fungal affected
422 (lower GR), indicating cellular alterations affecting their vital activity. This was clearly
423 observed in *A. alternata* and less noticeable in *B. fuckeliana*, which in turn exhibited
424 greater sensitivity to the active EO.
425 In *A. alternata*, an effect of the film's matrix composition (9:1 or 8:2 S:G ratio) was
426 observed both in the control samples and active films. The higher content of starch

14

427 enhanced fungal growth, limiting the action of EO in the cases where films contained a
428 low content of the active. At a higher EO content, the effect of the matrix was less
429 remarkable. This could be clearly seen when the GR and t_0 values were correlated with
430 the real content of EO in the films (Figure 4). In particular, two different relationships
431 could be observed between the t_0 values and the EO content in the film for the two
432 matrices. In 9:1 S:G matrices, a good linear correlation of t_0 and EC content was observed,
433 whereas more fluctuating, generally higher values were observed for 8:2 S:G films. This
434 also points to the nutritional effect of film starch on the fungi, which enhanced their
435 vitality and defense against the antifungal compounds. GR fluctuated between 4-5 mm
436 day^{-1} when the EO content was lower than 6-7 % in the dried film and decreased sharply
437 to 1-2 mm day^{-1} for higher contents of the EO. This suggests that the films require
438 relatively high contents of EO to ensure a good antifungal action against *A. alternata*.
439 These concentrations were only reached when lecithin encapsulation was used to prevent
440 losses of the EO during the film drying step or when the S:G ratio was 8:2 in the matrix
441 and EO was incorporated at the highest ratio (0.5 with respect to the polymer in the initial
442 dispersion). The best fungal control was achieved with the 9:1 (S:G) film formulation,
443 with lecithin-encapsulated EO (at a nominal ratio of 0.5), which retained the highest EO
444 content in the film matrix.
445 In the case of *B. fuckeliana*, all the films with EO content $\geq$ 0.074 g/g dried film
446 completely inhibited the growth of the fungus. At lower levels of EO, similar tendencies
447 to those commented on above for *A. alternata* were observed, although the nutritional
448 effect of starch on the fungus was scarcely noticeable when films contained EO, probably
449 due to the greater sensitivity of this fungus to the antifungal action of the EO. A linear
450 relationship could be observed for t_0 vs. EO content for all of the active films, the slope
451 being higher than that obtained for *A. alternata*, in line with the greater fungus sensitivity,
452 with small differences between the matrices with different starch ratios or the presence of
453 lecithin. Likewise, the GR fluctuated from 0.7 to 2.5 mm day^{-1} as a function of the EO
454 content in the film and the starch ratio in the matrix. The higher the EO content and the
455 lower the starch ratio, the lower the GR values. Of the film formulations allowing fungal
456 growth, the one containing 0.25 lecithin-encapsulated EO in an 8:2 S:G matrix was the
457 most effective at controlling the fungal development, despite this film retaining a slightly
458 lower amount of the EO than the corresponding 9:1 S:G film, thus reflecting the role
459 starch plays in the protection of the fungus's vitality.

Table 4. Slope (growth rate: GR, mm day^{-1}), intercept of the straight lines and estimated value of the total inhibition period (t_0, days) for *Alternaria alternata* (AA) and *Botryotinia fuckeliana* (BF). Mycelial growth inhibition (MGI, % values) at 7 days was also included.

Sample	*Alternaria alternata*				*Botryotinia fuckeliana*			
	GR (slope)	Intercept	t_0	MGI	GR (slope)	Intercept	t_0	MGI
9:1 (*Control*)	5.3 (0.2)	-0.4 (0.9)	0.07	-	2.2 (0.1)	0.3 (0.5)	-	
9:1-0.25	5.2 (0.1)	-3.8 (0.7)	0.73	9.9	2.5 (0.2)	-2.9 (0.9)	1.13	2.4
9:1-0.5	4.6 (0.1)	-7.6 (0.6)	1.65	28.8	1.1 (0.1)	-1.0 (0.3)	0.90	58.0
9:1-L (*Control*)	4.8 (0.1)	-0.9 (0.4)	0.19	-	1.8 (0.1)	2.9 (0.3)	-	
9:1-0.25-L	4.6 (0.2)	-8.8 (0.9)	1.91	24.9	1.8 (0.2)	-5.5 (0.9)	3.05	48.7
9:1-0.5-L	0.9 (0.9)	-3.3 (5.6)	3.51	89.6	-	-	-	100
8:2 (*Control*)	4.9 (0.1)	-1.5 (0.4)	0.31	-	2.2 (0.1)	0.4 (0.4)	-	
8:2-0.25	4.7 (0.1)	-4.2 (0.4)	0.90	10.5	1.8 (0.1)	-0.2 (0.7)	0.11	22.8
8:2-0.5	2.2 (0.5)	-5.6 (3.1)	2.59	67.5	-	-	-	100
8:2-L (*Control*)	4.9 (0.1)	-1.6 (0.4)	0.32	-	2.1 (0.1)	0.5 (0.4)	-	
8:2-0.25-L	4.3 (0.6)	-16.6 (3.9)	3.90	59.2	0.7 (0.2)	-1.3 (1.2)	1.92	75.3
8:2-0.5-L	2.0 (0.5)	-7.5 (3.2)	3.72	77.4	-	-	-	100

4. Conclusions

Starch-gellan blend films containing thyme essential oil (EO) exhibited antifungal effect in *in vitro* tests against *Alternaria alternata* (AA) and *Botryotinia fuckeliana* (BF), the second being more sensitive to the action of the EO. The antifungal action was correlated with the residual content of the oil in the film after the drying step and was slightly affected by the polymer matrix composition (9:1 or 8:2 S:G ratio). A greater amount of starch in the film protected the fungi, making their growth faster, when the active content was relatively low. The growth of AA was greatly inhibited when the EO content exceeded 0.05 g/g film, whereas BF was completely inhibited when films contained more than 0.053 g EO/ g film. Lecithin encapsulation of the EO greatly contributed to the EO retention in the film during film formation, which enhanced the film's antifungal action. Therefore, lecithin enhanced the film's water barrier properties, whereas all of the films exhibited high oxygen barrier capacity. Lecithin imparted a slightly brownish color to the films, but improved their gloss while reducing film stiffness and resistance to break and extensibility. Then, films with lecithin-encapsulated EO, with a S:G ratio of 8:2 were very effective at controlling fungal growth, while exhibiting adequate functional properties as packaging/coating materials.

16

References

Acosta, S., Chiralt, A., Santamarina, P., Rosello, J., González-Martínez, C., & Cháfer, M. (2016). Antifungal films based on starch-gelatin blend, containing essential oils. *Food Hydrocolloids*, *61*, 233–240. https://doi.org/10.1016/j.foodhyd.2016.05.008

Acosta, S., Jiménez, A., Cháfer, M., González-Martínez, C., & Chiralt, A. (2015). Physical properties and stability of starch-gelatin based films as affected by the addition of esters of fatty acids. *Food Hydrocolloids*, *49*, 135–143. https://doi.org/10.1016/j.foodhyd.2015.03.015

ASTM. (1995). Standard test methods for water vapour transmission of materials. Standard Designations: E96-95. In Annual book of ASTM standards. Philadelphia, PA: American Society for Testing and Materials.

ASTM. (1999). Standard test method for specular gloss. Standard Designations: D523. In Annual book of ASTM standards. Philadelphia, PA: American Society for Testing and Materials.

ASTM. (2001). Standard test method for tensile properties of thin plastic sheeting. Standard Designations: D882. In Annual book of ASTM standards. Philadelphia, PA: American Society for Testing and Materials.

ASTM. (2002). Standard test method for oxygen gas transmission rate through plastic film and sheeting using a colourimetric sensor. Standard Designations: 3985-95. In Annual book of ASTM standards. Philadelphia, PA: American Society for Testing and Materials.

Atarés, L., & Chiralt, A. (2016). Essential oils as additives in biodegradable films and coatings for active food packaging. *Trends in Food Science and Technology*, *48*, 51–62. https://doi.org/10.1016/j.tifs.2015.12.001

Bertan, L. C., Tanada-Palmu, P. S., Siani, A. C., & Grosso, C. R. F. (2005). Effect of fatty acids and "Brazilian elemi" on composite films based on gelatin. *Food Hydrocolloids*, *19*(1), 73–82. https://doi.org/10.1016/j.foodhyd.2004.04.017

Boubaker, H., Karim, H., El Hamdaoui, A., Msanda, F., Leach, D., Bombarda, I., Ait Ben Aoumar, A. (2016). Chemical characterization and antifungal activities of four

517   Thymus species essential oils against postharvest fungal pathogens of citrus.

518   *Industrial Crops and Products*, *86*, 95–101.

519   https://doi.org/10.1016/j.indcrop.2016.03.036

520 Calo, J. R., Crandall, P. G., O'Bryan, C. A., & Ricke, S. C. (2015). Essential oils as

521   antimicrobials in food systems - A review. *Food Control*, *54*, 111–119.

522   https://doi.org/10.1016/j.foodcont.2014.12.040

523 Cano, A., Jiménez, A., Cháfer, M., Gónzalez, C., & Chiralt, A. (2014). Effect of

524   amylose:amylopectin ratio and rice bran addition on starch films properties.

525   *Carbohydrate Polymers*, *111*, 543–555.

526   https://doi.org/http://dx.doi.org/10.1016/j.carbpol.2014.04.075

527 Cano, A., Fortunati, E., Cháfer, M., Kenny, J. M., Chiralt, A., & González-Martínez, C.

528   (2015). Properties and ageing behaviour of pea starch films as affected by blend with

529   poly(vinyl alcohol). *Food Hydrocolloids*, *48*, 84–93.

530   https://doi.org/10.1016/j.foodhyd.2015.01.008

531 Chandrasekaran, R., & Radha, A. (1995). Molecular architectures and functional

532   properties of gellan gum and related polysaccharides. *Trends in Food Science and*

533   *Technology*, *6*(5), 143–148. https://doi.org/10.1016/S0924-2244(00)89022-6

534 Espitia, P. J. P., Avena-Bustillos, R. J., Du, W. X., Chiou, B. Sen, Williams, T. G., Wood,

535   D., Soares, N. F. F. (2014). Physical and antibacterial properties of açaí edible films

536   formulated with thyme essential oil and apple skin polyphenols. *Journal of Food*

537   *Science*, *79*(5). https://doi.org/10.1111/1750-3841.12432

538 Fabra, M. J., Jimenez, A., Atares, L., Talens, P., & Chiralt, A. (2009). Effect of Fatty

539   Acids and Beeswax Addition on Properties of Sodium Caseinate Dispersions and

540   Films. *Biomacromolecules*, *10*(6), 1500–1507. https://doi.org/10.1021/bm900098p

541 Fabra, M. J., Pérez-Masiá, R., Talens, P., & Chiralt, A. (2011). Influence of the

542   homogenization conditions and lipid self-association on properties of sodium

543   caseinate based films containing oleic and stearic acids. *Food Hydrocolloids*, *25*(5),

544   1112–1121. https://doi.org/10.1016/j.foodhyd.2010.10.008

545 Fialho, A. M., Moreira, L. M., Granja, A. T., Popescu, A. O., Hoffmann, K., & Sá-

546   Correia, I. (2008). Occurrence, production, and applications of gellan: Current state

547   and perspectives. *Applied Microbiology and Biotechnology*, *79*(6), 889–900.

548   https://doi.org/10.1007/s00253-008-1496-0

549 Forssell, P., Lahtinen, R., Lahelin, M., & Myllärinen, P. (2002). Oxygen permeability of
550   amylose and amylopectin films. *Carbohydrate Polymers*, *47*(2), 125–129.
551   https://doi.org/10.1016/S0144-8617(01)00175-8

552 Ghanbarzadeh, B., Almasi, H., & Entezami, A. A. (2011). Improving the barrier and
553   mechanical properties of corn starch-based edible films : Effect of citric acid and
554   carboxymethyl cellulose. *Industrial Crops & Products*, *33*(1), 229–235.
555   https://doi.org/10.1016/j.indcrop.2010.10.016

556 Jiménez, A., Fabra, M. J., Talens, P., & Chiralt, A. (2012). Effect of re-crystallization on
557   tensile, optical and water vapour barrier properties of corn starch films containing
558   fatty acids. *Food Hydrocolloids*, *26*(1), 302–310.
559   https://doi.org/10.1016/j.foodhyd.2011.06.009

560 Jiménez, A., Sánchez-González, L., Desobry, S., Chiralt, A., & Tehrany, E. A. (2014).
561   Influence of nanoliposomes incorporation on properties of film forming dispersions
562   and films based on corn starch and sodium caseinate. *Food Hydrocolloids*, *35*, 159–
563   169. https://doi.org/10.1016/j.foodhyd.2013.05.006

564 Jouki, M., Mortazavi, S. A., Yazdi, F. T., & Koocheki, A. (2014). Characterization of
565   antioxidant-antibacterial quince seed mucilage films containing thyme essential oil.
566   *Carbohydrate Polymers*, *99*, 537–546.
567   https://doi.org/10.1016/j.carbpol.2013.08.077

568 Kim, S. R. B., Choi, Y. G., Kim, J. Y., & Lim, S. T. (2014). Improvement of water
569   solubility and humidity stability of tapioca starch film by incorporating various
570   gums. *LWT - Food Science and Technology*, *64*(1), 475–482.
571   https://doi.org/10.1016/j.lwt.2015.05.009

572 Krog, N. J. (1990). Food emulsifiers and their chemical and physical properties, in *Food
573   emulsions*. (K. Larsson & S. E. Friberg, Eds.) (2nd ed.). New York and Basel: Marcel
574   Dekker, Inc.

575 Larsson, K., & Dejmek, P. (1990). Crystal and liquid crystal structures of lipids, in *Food
576   emulsions*. (K. Larsson & S. E. Friberg, Eds.) (2nd ed.). New York and Basel: Marcel
577   Dekker, Inc.

578 Luchese, C. L., Spada, J. C., & Tessaro, I. C. (2017). Starch content affects
579   physicochemical properties of corn and cassava starch-based films. *Industrial Crops
580   and Products*, *109*(May), 619–626. https://doi.org/10.1016/j.indcrop.2017.09.020

581 McHugh, T. H., Avena-Bustillos, R., & Krochta, J. M. (1993). Hydrophilic Edible Films
582   - Modified Procedure for Water-Vapor Permeability and Explanation of Thickness

583   Effects. *J Food Sci*, *58*(4), 899–903. https://doi.org/10.1111/j.1365-
584   2621.1993.tb09387.x

585 Nieto, M. B. (2009). *Structure and Function of Polysaccharide Gum-Based Edible Films*
586   *and Coatings*. https://doi.org/10.1007/978-0-387-92824-1

587 Núñez-Flores, R., Giménez, B., Fernández-Martín, F., López-Caballero, M. E., Montero,
588   M. P., & Gómez-Guillén, M. C. (2012). Role of lignosulphonate in properties of fish
589   gelatin films. *Food Hydrocolloids*, *27*(1), 60–71.
590   https://doi.org/10.1016/j.foodhyd.2011.08.015

591 Ojagh, S. M., Rezaei, M., Razavi, S. H., & Hosseini, S. M. H. (2010). Development and
592   evaluation of a novel biodegradable film made from chitosan and cinnamon essential
593   oil with low affinity toward water. *Food Chemistry*, *122*(1), 161–166.
594   https://doi.org/10.1016/j.foodchem.2010.02.033

595 Parra, D. F., Tadini, C. C., Ponce, P., & Lugão, A. B. (2004). Mechanical properties and
596   water vapor transmission in some blends of cassava starch edible films.
597   *Carbohydrate Polymers*, *58*(4), 475–481.
598   https://doi.org/http://dx.doi.org/10.1016/j.carbpol.2004.08.021

599 Perdones, Á., Chiralt, A., & Vargas, M. (2016). Properties of film-forming dispersions
600   and films based on chitosan containing basil or thyme essential oil. *Food*
601   *Hydrocolloids*, *57*, 271–279. https://doi.org/10.1016/j.foodhyd.2016.02.006

602 Ruiz-Navajas, Y., Viuda-Martos, M., Sendra, E., Perez-Alvarez, J. A., & Fernández-
603   López, J. (2013). In vitro antibacterial and antioxidant properties of chitosan edible
604   films incorporated with Thymus moroderi or Thymus piperella essential oils. *Food*
605   *Control*, *30*(2), 386–392. https://doi.org/10.1016/j.foodcont.2012.07.052

606 Sánchez-González, L., Vargas, M., González-Martínez, C., Chiralt, A., & Cháfer, M.
607   (2009). Characterization of edible films based on hydroxypropylmethylcellulose and
608   tea tree essential oil. *Food Hydrocolloids*, *23*(8), 2102–2109.
609   https://doi.org/10.1016/j.foodhyd.2009.05.006

610 Santamarina, M. P., Ibáñez, M., Marqués, M., Roselló, J., Giménez, S., & Blázquez, M.
611   A. (2016). Bioactivity of essential oils in phytopathogenic and post-harvest fungi
612   control. *Natural Product Research*, *31*(22), 2675–2679.
613   https://doi.org/https://doi.org/10.1080/14786419.2017.1286479

614 Santamarina, M. P., Roselló, J., Giménez, S., & Blázquez, M. A. (2016). Commercial
615   Laurus nobilis L. and Syzygium aromaticum L. Merr. & Perry essential oils against

616   post-harvest phytopathogenic fungi on rice. *LWT - Food Science and Technology*,

617   *65*, 325–332. https://doi.org/10.1016/j.lwt.2015.08.040

618 Song, X., Zuo, G., & Chen, F. (2018). Effect of essential oil and surfactant on the physical

619   and antimicrobial properties of corn and wheat starch films. *International Journal*

620   *of Biological Macromolecules*, *107*, 1302–1309.

621   https://doi.org/10.1016/j.ijbiomac.2017.09.114

622 Souza, A. C., Goto, G. E. O., Mainardi, J. A., Coelho, A. C. V, & Tadini, C. C. (2013).

623   Cassava starch composite films incorporated with cinnamon essential oil:

624   Antimicrobial activity, microstructure, mechanical and barrier properties. *LWT -*

625   *Food Science and Technology*, *54*(2), 346–352.

626   https://doi.org/10.1016/j.lwt.2013.06.017

627 Tampau, A., González-Martinez, C., & Chiralt, A. (2017). Carvacrol encapsulation in

628   starch or PCL based matrices by electrospinning. *Journal of Food Engineering*, *214*,

629   245–256. https://doi.org/10.1016/j.jfoodeng.2017.07.005

630 Valencia-Sullca, C., Jiménez, M., Jiménez, A., Atarés, L., Vargas, M., & Chiralt, A.

631   (2016). Influence of liposome encapsulated essential oils on properties of chitosan

632   films. *Polymer International*, *65*(8), 979–987. https://doi.org/10.1002/pi.5143

633 Xiao, G., Zhu, Y., Wang, L., You, Q., Huo, P., & You, Y. (2011). Production and storage

634   of edible film using gellan gum. *Procedia Environmental Sciences*, *8*(November),

635   756–763. https://doi.org/10.1016/j.proenv.2011.10.115

636 Yang, L., Paulson, A. T., & Nickerson, M. T. (2010). Mechanical and physical properties

637   of calcium-treated gellan films. *Food Research International*, *43*(5), 1439–1443.

638   https://doi.org/10.1016/j.foodres.2010.04.010

639 Zhang, H. Y., Arab Tehrany, E., Kahn, C. J. F., Ponot, M., Linder, M., & Cleymand, F.

640   (2012). Effects of nanoliposomes based on soya, rapeseed and fish lecithins on

641   chitosan thin films designed for tissue engineering. *Carbohydrate Polymers*, *88*(2),

642   618–627. https://doi.org/10.1016/j.carbpol.2012.01.007

643

644

645

646

647
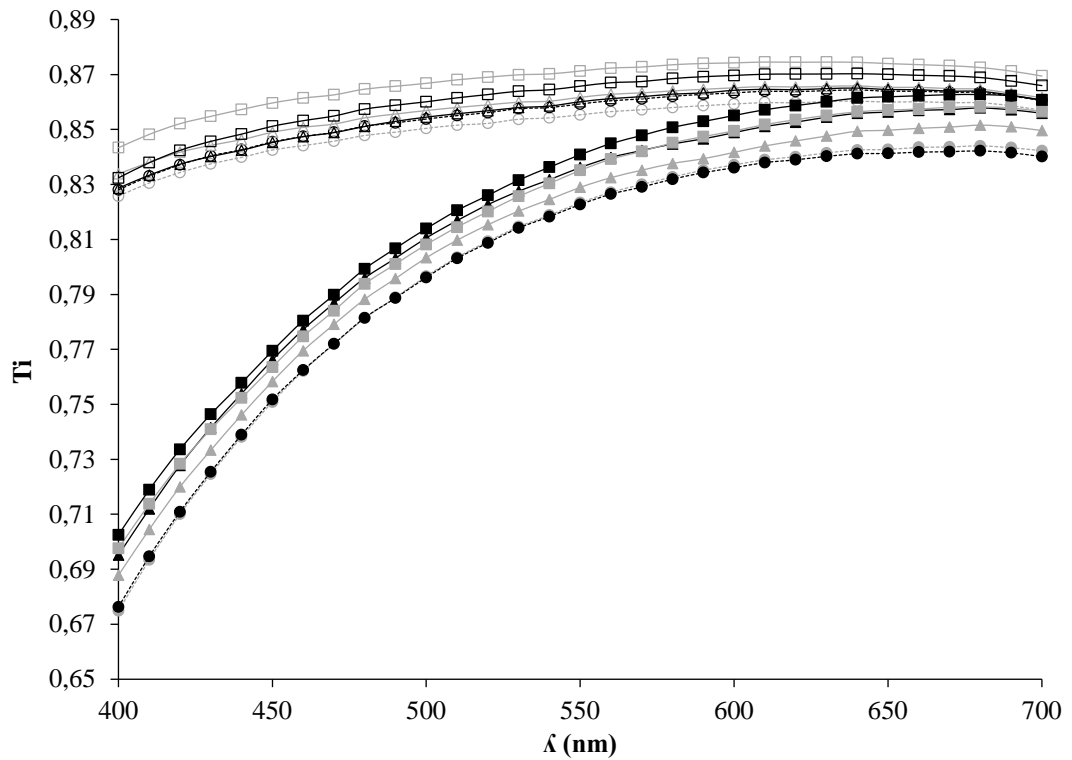
648
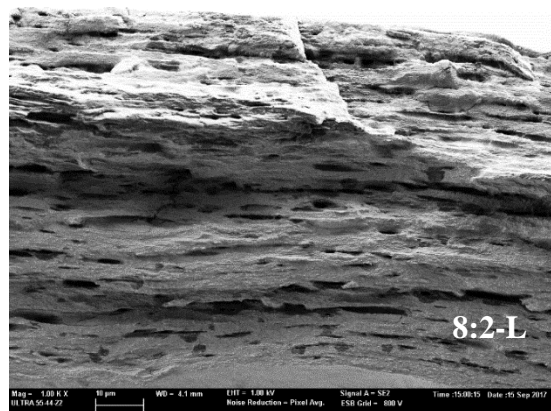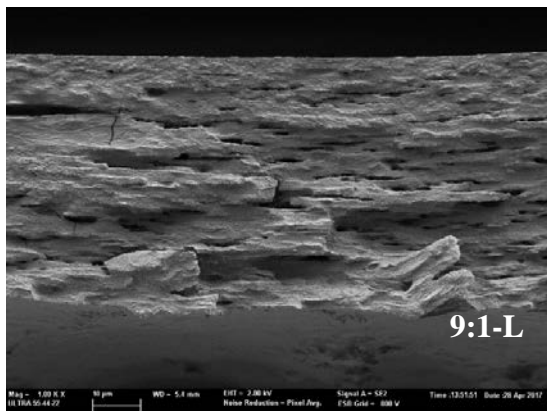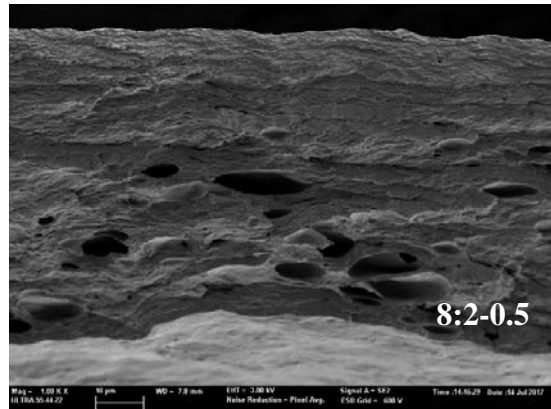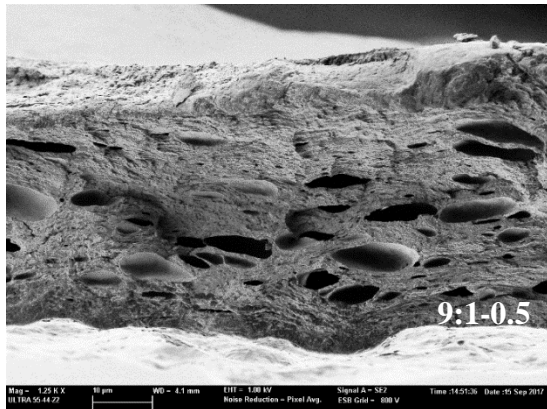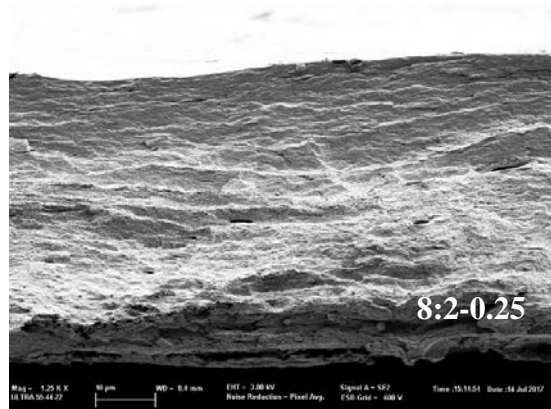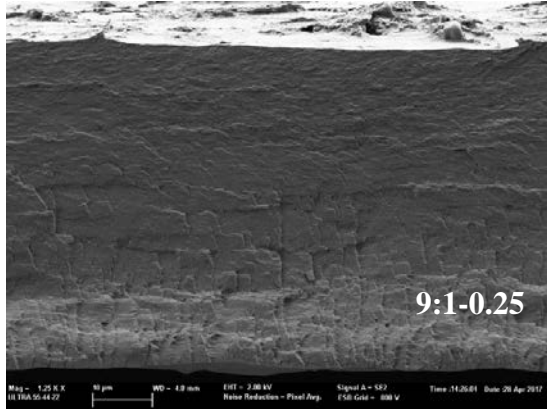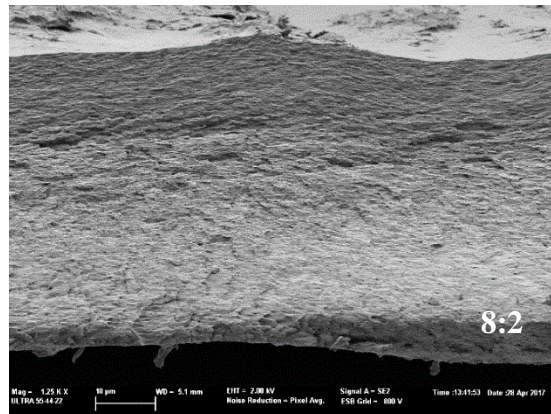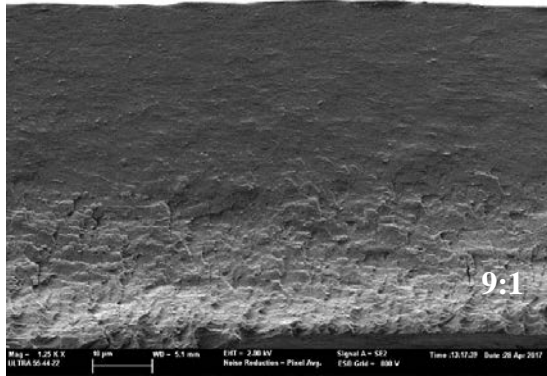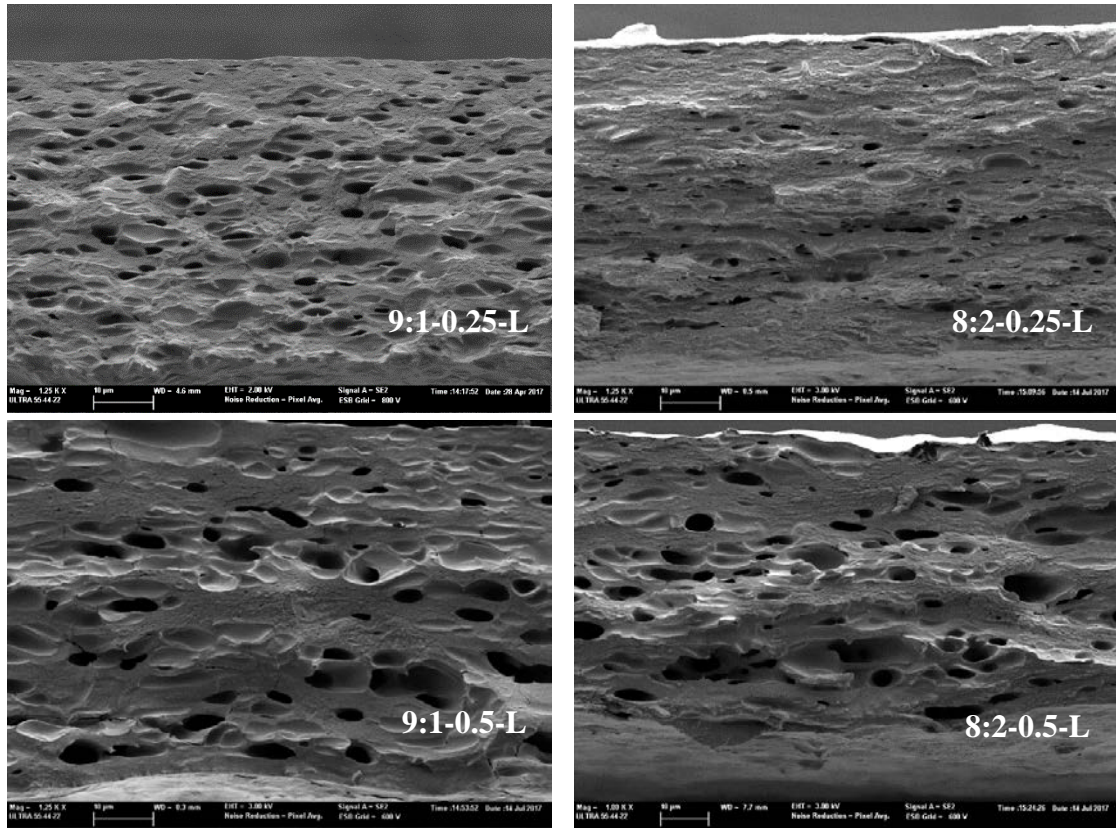
Fig. 1. FESEM micrographs of the cross-section of the starch-gellan films with and without EO in the formulations 9:1 (left) and 8:2 (right).

Fig. 2. Spectral distribution of internal transmittance (T_i) between 400 and 700 nm for every film formulation with different starch:gellan ratios (grey: 9:1, black: 8:2) containing EO (0.25 or 0.5 g/g polymer: triangle and square, respectively), emulsified (empty symbols) or lecithin-encapsulated (full symbols), and without EO (control: circles). Embedded table shows the T_i values at 400 nm and the ANOVA carried out separately for samples with and without lecithin. Different superscript letters within the same column indicate significant differences among films ($p < 0.05$).

701


Alternaria alternata

702

Botryotinia fuckeliana

703
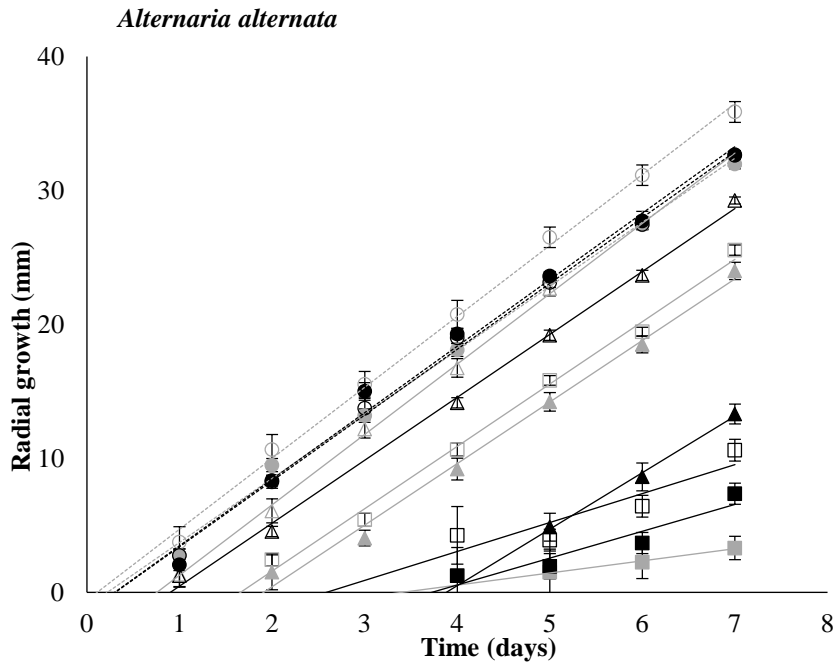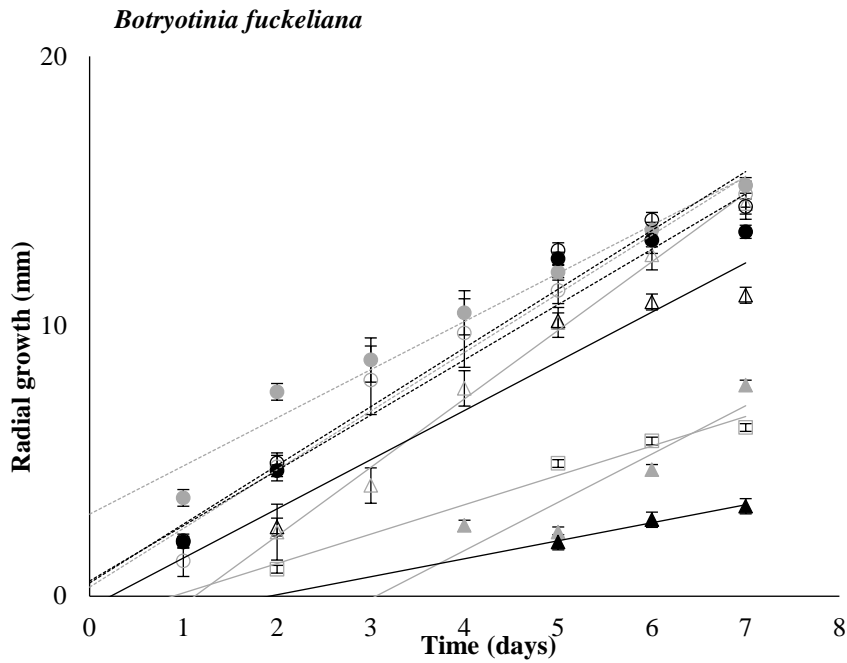
Fig. 3. Radial growth of *Alternaria alternata* (AA) and *Botryotinia fuckeliana* (BF) for
every film formulation with different starch:gellan ratios (grey: 9:1, black: 8:2) containing
EO (0.25 or 0.5 g EO/g polymer: triangles and squares, respectively), emulsified (empty
symbols) or lecithin-encapsulated (full symbols) and without EO (control: circles).

708

709
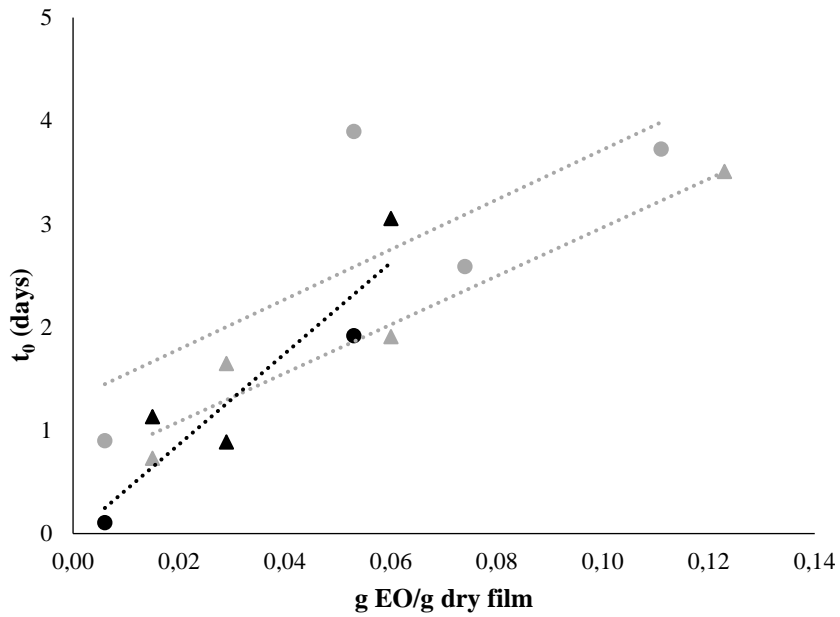
710

25

711

712

713
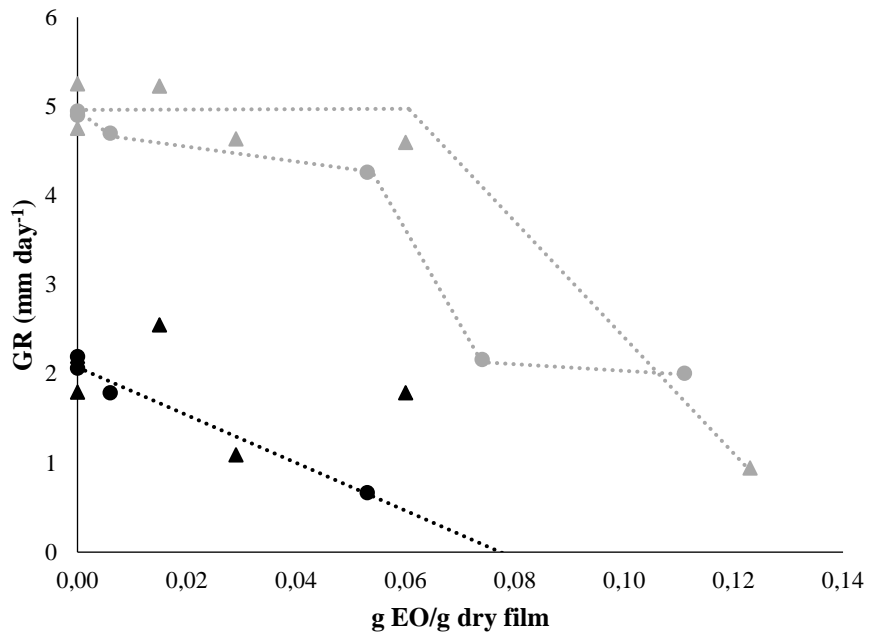
Fig. 4. Relationships between GR and t_0 with the actual EO concentration in the films with different S:G ratios (9:1:, triangles, 8:2: circles) for both fungi (AA: grey and BF: black).

717